Circadian oscillations persist in cervical and esophageal cancer cells displaying decreased expression of tumor-suppressing circadian clock genes

Watt, P. J. V. D., Roden, L., Davis, K., Parker, M. I. & Leaner, V. D.

Original citation & hyperlink:
Watt, PJVD, Roden, L, Davis, K, Parker, MI & Leaner, VD 2020, 'Circadian oscillations persist in cervical and esophageal cancer cells displaying decreased expression of tumor-suppressing circadian clock genes', Molecular Cancer Research, vol. 18, no. 9, MCR-19-1074R, pp. 1340-1353.
https://dx.doi.org/10.1158/1541-7786.MCR-19-1074

DOI 10.1158/1541-7786.MCR-19-1074
ISSN 1541-7786
ESSN 1557-3125

Publisher: American Association for Cancer Research

Circadian clock genes are rhythmically expressed but downregulated in cervical cancer and oesophageal cancer cells and act to repress cancer cell proliferation

van der Watt P.J.[1]*, Roden L.C.[3], Davis K[1], Parker, M.I. [1#] and Leaner V.D[1,2#].

[1]Division of Medical Biochemistry and Structural Biology, Department of Integrative Biomedical Sciences, [#]Institute of Infectious Disease and Molecular Medicine, [2]SAMRC/UCT Gynaecological Cancer Research Centre, Faculty of Health Sciences, University of Cape Town, South Africa; [3]School of Life Sciences, Coventry University, Coventry, CV1 2DS, United Kingdom

Keywords: circadian clock, cancer, tumour suppressor

Running title: Circadian clock genes associate with cancer

*Correspondence to:

Pauline van der Watt

Division of Medical Biochemistry and Structural Biology

Department of Integrative Biomedical Sciences

Faculty of Health Sciences, University of Cape Town

Observatory, Cape Town, 7925, South Africa

Ph: 27 21 406 6266; Pauline.vanderwatt@uct.ac.za

Disclosure of Potential Conflicts of Interest

The authors declare no potential conflicts of interest.

Abstract

There is accumulating evidence for a link between circadian clock disruption and cancer progression. In this study, the circadian clock was investigated in cervical and oesophageal cancers, to determine whether it is disrupted in these cancer types. Oncomine data-mining revealed simultaneous downregulation of multiple members of the circadian clock gene family in cervical cancer and oesophageal cancer patient tissue compared to matched normal epithelium. Real-time RT-PCR analysis confirmed significant downregulation of *Clock, Per1, Per2, Per3, Cry1, Cry2* and *Rev-erbα* and *RORα* in oesophageal tumour tissue. In cell line models, expression of several circadian clock gene family members was significantly decreased in transformed and cancer cells compared to non-cancer controls, and protein levels were also dysregulated. These effects were mediated at least in part by methylation, where promoter regions of the *Clock*, *Cry1* and *RORα* genes were found to be methylated in cancer cells. Overexpression of *Clock* and *Per2* in cancer cell lines negatively affected cell proliferation, and activation of *RORα* and *Rev-erbα* using agonists resulted in cancer cell death, while having a lesser effect on normal epithelial cells. Despite dysregulated circadian clock gene expression, cervical and oesophageal cancer cells maintain functional circadian oscillations after synchronisation with Dexamethasone, as revealed using real-time bioluminescence imaging, suggesting that their circadian clock mechanisms are still intact. Together, this study is a first to describe dysregulated circadian clock gene expression in cervical and oesophageal cancer, although cells maintain a functional circadian rhythm. Elucidating differences in circadian clock functioning in normal and cancer cells could yield important insights into the timing of administration of chemotherapy, ultimately ensuring a better patient response.

Introduction

The circadian clock aligns metabolic and physiological processes, at cellular and systemic levels, to the external light and dark 24 hour cycle. At the molecular level, the circadian clock comprises a core set of rhythmically expressed genes and gene products, *Bmal1, Clock, Cryptochrome (Cry), Period (Per), Rev-erb* and *ROR*, that drive rhythmic expression of clock-controlled genes to generate overt circadian rhythms [1]. Clock and Bmal1 proteins heterodimerise and activate the expression of *Cry* and *Per* genes, which once translated in the cytoplasm repress Clock/Bmal1 activity to inhibit their own transcription [1]. Bmal1 levels are further controlled by negative and positive regulatory transcription factors, Rev-erbα/β and RORα [1]. All nucleated cells harbour a circadian clock mechanism and express circadian clock genes [2]. The suprachiasmatic nucleus (SCN) is the master clock in the brain which receives light signals via the retino-hypothalamic tract and generates neural and hormonal signals accordingly [2]. This is turn synchronises peripheral clocks, which are those molecular clock networks expressed in all non-SCN cell types. Up to 40 % of the genome is regulated in a circadian fashion, highlighting the crucial role of the circadian clock in cell biology [3]. Its dysregulation is implicated in several disease states, including cancer.

Circadian disruption has been correlated with increased cancer risk and progression. This correlation has been evident in shift workers and the International Agency for Research on Cancer (IARC) classified shiftwork that results in circadian disruption as a probable carcinogen (group 2A carcinogen) [4]. With recent epidemiological data suggesting that more than 80 % of the population may be living a lifestyle of chronic circadian disruption, this has widespread implications [5]. In mouse studies, disruption of the light cycle accelerates tumourigenesis [6] and meal timing inhibits cancer growth by approximately 40 %, as compared with mice fed *ad libitum* [7]. Interestingly, studies have shown that cancer cells in general

commonly display a disrupted circadian rhythm or exhibit deregulated circadian clock gene expression [8], where for example loss of circadian clock gene expression has been correlated with poor prognosis in various cancer types [9,10,11,12]. It has recently been shown that tumour hypoxia aggravates the extent of circadian dysregulation [13]. Furthermore, a link between metabolic perturbations of cancer cells and circadian clock disruption has been described [14]. These studies highlight how the circadian clock is entwined in important cellular processes implicated in cancer development.

While disruptions in the circadian clock have been described in certain cancers, there are no documented reports to date on the circadian machinery of cervical cancer or oesophageal cancer cells, and with these cancer types being prevalent in the developing world they require further investigation. Cervical cancer was classified as the fourth most common cancer among women worldwide in 2018, and the second most common cancer among women in countries with a low human development index (HDI) (GLOBOCAN 2018, IARC) [15]. Oesophageal cancer was classified as the seventh most common cancer among men worldwide in 2018, and the sixth most common cancer among men and seventh among women in countries with a low HDI [15]. Knowledge of circadian clock functioning in these cancer types could provide important information to benefit diagnosis and treatment. In particular, with many drug targets and drug metabolising enzymes expression in a circadian fashion, knowledge of the circadian rhythm exhibited by cancer cells can inform when to optimally administer chemotherapy, enhancing its efficacy and minimising toxicity.

In this study we show that expression of multiple circadian clock genes is downregulated in cervical and oesophageal cancer cells. These cells however, maintain functional circadian oscillations. Furthermore, we show that interfering with circadian clock expression/activity in these cancer types has an inhibitory

effect on cancer biology. It has been reported that circadian clock genes are potential “druggable” targets, due to their dysregulation in cancer cells [5]. Our study supports further investigation into the targeting of circadian clock machinery as an anti-cancer strategy.

Methods

Cell lines and cell culture

Human primary and immortalized retinal epithelial cell lines, ARPE19 and hTERT-RPE-1, respectively, were cultured in DMEM:F12 (Gibco) supplemented with 10 % fetal bovine serum (FBS, Gibco) and penicillin and streptomycin. hTERT-RPE-1 media was supplemented with 0.01 mg/ml Hygromycin B. Human fibroblasts (WI38 and SVWI38), cervical cancer cell lines (HeLa, CaSki and ME180), oesophageal cancer cell lines (WHCO1, WHCO5 and KYSE30), and osteosarcoma cell line (U2OS) were maintained in DMEM (Gibco) supplemented with 10 % fetal bovine serum and penicillin and streptomycin. All cells except U2OS cells, which were kindly provided by Prof. J. Hapgood, University of Cape Town, were obtained from the ATCC. Cells were maintained in a humidified incubator at 37°C and in 5 % carbon dioxide. Cancer cell lines were authenticated by DNA profiling using the Cell ID system (Promega).

Stable cell lines were generated using the Tol2 transposon system as described by Yagita et al., 2010 [16]. The *Per2* promoter fused to destabilized luciferase (*Per2-dLuc*) was kindly provided by Prof. K. Yagita (Kyoto Prefectural University of Medicine, Japan). The *Bmal1-dLuc* construct was generated by excising the *Bmal1* promoter-luciferase construct from the pGL4.27 plasmid, kindly provided by Dr J. Hogenesch (University of Pennsylvania, USA) [17], and inserting it into the Tol2 plasmid. Cells were transfected using Genecellin (Celtic Diagnostics) and stable *Per2-dLuc*- or *Bmal1-dLuc*-expressing cells selected for in media containing between 100 and 500 µg/ml Zeocin (Invitrogen).

Cells were treated with RORα agonist, SR1078 (Merck), Rev-erbα agonist, SR9011 (Sigma), and the methylation inhibitor, 5-aza-2-deoxycytidine (Sigma), dissolved in DMSO. Drug stocks were prepared at concentrations of 5 mM, 4.175 mM and 10 mM, respectively, and stored at -20°C.

Clinical specimens

24 pairs of freshly frozen normal oesophageal epithelial and oesophageal cancer samples, and 8 freshly frozen normal cervical epithelial and 16 cervical cancer samples, were obtained from patients at Groote Schuur and Tygerberg hospitals and RNA extracted. Time of tissue collection was important in a study examining the circadian clock: all cervical specimens (normal and cancer) were collected during the morning (between 8 am and midday) so at an approximately equivalent time of day, and since oesophageal specimens comprised normal and cancer epithelial tissue, matched normal and cancer samples were from the same time of day. This study was authorized by the University of Cape Town Research Ethics Committee (REC REF: 153/2004 and 040/2005), and written informed consents were provided by all patients for using their biopsy tissue samples.

Plasmids

Overexpression plasmids were obtained as follows: myc-tagged mPer2 (pCS2+mt-6myc-mPER2) was kindly provided by Prof. David Virshup (Duke-MED Medical School, Singapore) [18], flag-tagged mClock (pCMV10/3Xflag-Clock) was purchased from Addgene and a kind gift from Joseph Takahashi (Addgene plasmid #47334) [19], flag-, myc- and his-tagged hCry1 in pcDNA4 (pfmh-hCry1) was purchased from Addgene and a kind gift from Aziz Sancar (Addgene plasmid #25843), and Venus-tagged mBmal1 (pcDNA3.1-Venus-mBmal1) was kindly provided by Prof. Kyungjin Kim (University of Pennsylvania School of Medicine, USA) [20]. Empty vector controls were generated by excising the circadian clock genes from

their respective plasmids, and religation using the Quick Blunting and Quick Ligation kits (New England Biolabs).

RNA extraction and reverse transcription quantitative PCR (RT-qPCR)

Total RNA was extracted from patient tissue and cultured cell lines (2 hours after Dexamethasone synchronisation) using Qiazol Reagent (Qiagen) according to the manufacturer's instructions. RNA was reverse-transcribed to cDNA with ImPromII reverse transcriptase (Promega). Quantitative PCR reactions were performed using the Kapa Fast SYBR Green qPCR reagent (Kapa Biosystems), using the following primers: Clock forward, 5'-GTAGCTTGTGGGGCAGTCAT-3' and reverse, 5'-TGGAGCAACCTAGAAGTCTGT-3'; Bmal1 forward, 5'-ATTCTTGGTGAGAACCCCCAC-3' and reverse, 5'-TGTAGTGTTTACAGCGGCCA-3', Cry1 forward, 5'-GCAGTTGCTTGCTTCCTGAC-3' and reverse, 5'-GACAGGCAAATAACGCCTGA-3', Cry2 forward, 5'-CCTGAGACTGCAGAGCCCTT-3' and reverse, 5'-CTGGCGTGCTACAGGTACTC-3', Per1 forward, 5'-AGGATCCCATTTGGCTGCTC-3' and reverse, 5'-TCCACACAGGCCATCACAT-3', Per2 forward, 5'-ATCGACGTGGCAGAATGTGT-3' and reverse, 5'-TCTCTTCCAAGCACCACCTG-3', Per3 forward, 5'-AGACACCTGAGCGCATTCTC-3' and reverse, 5'-GTGACACAGGCTTGAATGTCG-3', RORα forward, 5'-AGCAGATCGCTCATGGCTG-3' and reverse, 5'-GAAGTCGCACAATGTCTGGG-3', RORβ forward, 5'-CTGATATCTCCAGACCGAGCC-3' and reverse, 5'-CAAACTGCCGTGATGGTTGG-3', RORγ forward, 5'-GAAGTGACTGGCTACCAGAGG-3' and reverse, 5'-CACTTCCATTGCTCCTGCTTTG-3', Rev-erbα forward, 5'-CTTTGAGGTGCTGATGGTGCG-3' and reverse, 5'-CACCGAAGCGGAATTCTCCA-3', Rev-erbβ forward, 5'-GGAGGAAGAATGCATCTGGTTTG-3' and reverse, 5'-GAACCCAGGAATACGCTTTGC-3', GAPDH forward, 5'-GGCTCTCCAGAACATCATCC-3' and reverse, 5'-GCCTGCTTCACCACCTTC-3', β-glucuronidase forward, 5'-CTCATTTGGAATTTTGCCGATT-3' and reverse, 5'-CCGAGTGAAGATCCCCTTTTTA-3' and Cyclophilin D forward, 5'-TGAGACAGCAGATAGAGCCAAGC-3' and reverse, 5'-TCCCTGCCAATTTGACATCTTC-3' were

applied as the endogenous controls for normalization, and the 2-△△CT was used to calculate the relative mRNA expression [21].

Western blot analysis

Protein was extracted from cells 2 hours after synchronisation with Dexamethasone, using RIPA lysis buffer and the Bicinchoninic acid (BCA) assay kit (Pierce) used to determine protein concentration. A total of 20µg protein was separated by SDS-polyacrylamide gel electrophoresis (SDS-PAGE) and then transferred onto nitrocellulose membranes (Millipore). After transfer, the membrane was blocked in 5% skimmed milk for 1 h and then incubated with primary anti-Clock (1:2000; Pierce #PA1-520), anti-Bmal1 (1:2000; Abcam #ab93806), anti-Cry1 (1:1000; Santa Cruz Biotechnology #sc-33177), anti-Per2 (1:1000; Abcam #ab179813), anti-RORα (1:750; Abcam #ab70061), anti-Rev-erbα (1:500, Millipore #AB10130), or anti-p38 (1:5000, Sigma #M0800) antibody overnight at 4°C, followed by species-matched secondary antibodies for 1 h at room temperature. Finally, protein bands were visualized using Lumiglo detection reagent (Thermofisher). For Parp-1 cleavage analysis, protein was harvested from cells and cell floaters 72 hours after treatment with SR9011 or SR1078 using RIPA lyisis buffer and Western blot analysis performed, as above, using anti-Parp-1 (1:500; Santa Cruz Biotechnology #sc-7150) antibody overnight at 4°C.

Methylation-specific PCR

Bisulfite treatment of genomic DNA was carried out using the EpiTect Fast LyseAll Bisulfite Kit (Qiagen), according to the manufacturer's instructions. Bisulfite-modified DNA was then amplified by PCR using primer sets designed to detect either methylated or unmethylated DNA, designed using Methprimer,

and according to Davidovic et al. (2014) [22] (as listed in Table 1). PCR was carried out using 200 nM each primer, 200 µM dNTPs, 1.5 mM $MgCl_2$ 1.25 U GoTaq G2 Flexi DNA polymerase (Promega) and 100 ng bisulfite-converted DNA. Cycling conditions were: 95°C for 2 minutes, followed by 40 cycles of 95°C for 30 seconds, 52°C or 55°C (for unmethylated or methylated primer reactions, respectively), and 72°C for 30 seconds, followed by a final elongation step of 72°C for 5 minutes. The PCR products were visualized by 1.5 % agarose gel electrophoresis. CpG methylase (SssI)-treated sodium bisulfite-modified genomic DNA was used as a positive control for methylation-specific primers. To determine the effect of 5-aza-2-deoxycytidine on circadian clock gene promoter methylation, cells were treated with varying concentrations of 5-aza-2-deoxycytidine every day for 3 days, and the next day DNA harvested, and bisulfite converted. DNA amplification was then performed by real-time PCR, using the Kapa Fast SYBR Green qPCR reagent (Kapa Biosystems) and 250 nM each methylation-specific primer. PCR amplification was stopped before fluorescence generated from untreated cancer cell lines had reached saturation (or the "plateau effect"); that is at 35 cycles for *Clock* and 28 cycles for *RORα* and *Cry1*. PCR products were visualized by 1.5 % agarose gel electrophoresis.

MTT cell proliferation assays

5000 cells/well were plated in 96-well plates and the following day either transfected with overexpression plasmids, using Genecellin (Celtic Diagnostics), or treated with RORα/Rev-erbα agonists. Proliferation was assessed 3 to 4 days after treatment or transfection, respectively by addition of MTT in PBS at 5 mg/ml. After incubation at 37°C for 4 hours, MTT solvent was added and absorbance measured at 595 nm.

Trypan blue assays

Cells were plated in 24-well plates and treated with varying concentrations of RORα/Rev-erbα agonists for 72 hours. Following treatment, cell floaters and adherent cells were collected by trypsinization, stained using 0.4 % Trypan blue stain, and counted using a haemacytometer. Dead cells were counted as those cells that had stained blue, whereas live cells were those that had excluded the stain.

Caspase-Glo 3/7 assay

Cells were plated in 96-well plates and treated with RORα/Rev-erbα agonists for 72 hours, whereafter the Caspase-Glo 3/7 assay (Promega) was performed, according to the manufacturer's instructions. Luminescence was measured using the Veritas microplate luminometer (Promega) and normalised to OD595 readings of MTT experiments performed in parallel.

Real-time bioluminescence imaging

For imaging, 5000 *Per2-dLuc*- or *Bmal1-dLuc*-expressing cells were seeded in white 96-well plates with clear bottom. The next day cells were synchronized with Dexamethasone (Sigma) for 2 hours, following which media was replaced with Leibovitz L-15 (Thermofisher) containing 10 % FCS and 150 µg/ml D-Luciferin (Promega). Luciferase activity was measured using the IVIS Lumina II (PerkinElmer). Images were collected at intervals of 60 min, with 10 min exposure duration, for up to 4 days. Images were acquired using Living Image 3.2 Acquisition software (PerkinElmer), and analysed using Time Series Analysis 6.3 software (Expert Soft Tech.). Phase, period and amplitude were determined using detrended and smoothed bioluminescence data.

Statistical analysis

Statistical analyses were performed using Microsoft excel, where the student t-test was performed to assess differences in sample means and a p value of < 0.05 was considered statistically significant. For analysis of continuous luminometer readings, Time Series Analysis 6.3 software (Expert Soft Tech.) was used. Period was calculated using the Jenkin and Watts autoperiodogram test and cosinor curves generated using the population-mean cosinor method. Cosinor curves shown depict the mean of biological replicates.

Results

Circadian clock gene expression is downregulated in cervical and oesophageal cancer patient tissue

A microarray study we previously conducted, comparing the gene expression profiles of cervical tumour tissue and normal epithelial tissue from cervical cancer patients and healthy controls, identified the circadian clock gene, *Period 2 (Per2)*, as one of the most significantly differentially expressed genes in cervical cancer and normal cervical tissue [23,24]. Its expression was amongst the ten most significantly downregulated genes in cancer compared to normal (*$p < 0.0005$) (Suppl. fig. 1A). This downregulation of *Per2* suggests that the circadian clock is altered in cervical cancer. Data-mining of the Oncomine gene expression database, a platform aimed at facilitating discovery from genome-wide expression analyses [25], confirmed downregulation of *Per2* in cervical cancer tissue, and revealed significant downregulation of other core circadian clock genes, *Clock, Bmal1, Per1, Cry1, Rev-erbα* and *RORα* in high grade squamous intraepithelial lesion (HSIL) and/or cervical cancer tissue specimens compared to normal cervical epithelium, using data derived from two independent studies [26,27] (Fig. 1A). The downregulation of circadian clock genes in HSIL tissues suggests that deregulation of circadian clock gene expression occurs as an early rather than late event in disease progression (Fig. 1Aii). Similarly, circadian clock gene expression analysed using other valuable resources of gene expression data, The Cancer Genome Atlas (TCGA) and The Genotype Tissue Expression (GTEx) project, after removal of study-specific biases [28], revealed significant downregulation of several circadian clock genes in cervical tumour tissue compared to normal (Suppl. fig. 2A). *Bmal1* and *Clock* constitute the positive arm of the molecular circadian clock, and *Per* and *Cry* genes the negative arm. *RORα* and *Rev-erbα* positively and negatively regulate expression of *Bmal1*, respectively. In all datasets, positive and negative circadian clock genes were downregulated. To show that there was not global downregulation of all genes using data derived from TCGA and GTEx studies, expression of *Ki67* and *p16* was evaluated, and both were found to be at significantly increased levels in cervical cancer tissue compared to normal, as expected (Suppl. Fig. 2B).

Due to the observed downregulation of multiple members of the circadian clock gene family in cervical cancer tissue, circadian clock gene expression in oesophageal cancer patient tissue was next investigated by Oncomine-data mining, to determine whether this effect was specific to cervical cancer or a more general phenotype of cancer cells. Similar to the results obtained for cervical cancer, multiple circadian clock genes were found to be downregulated in oesophageal squamous cell carcinoma (OSCC) tumour tissue compared to matched normal epithelium in two independent datasets [29,30], including *Clock, Per1, Per2, Per3, Cry1, Cry2, Rev-erbα* and *RORα* genes (Fig. 1B). Circadian clock gene expression was similarly found to be downregulated in oesophageal tumour tissue compared to normal oesophageal epithelium, using data obtained from TCGA and GTEx project resources (Suppl. fig. 2C). Again, expression of *Ki67* was found to be at increased levels in the tumour tissue compared to normal, as well as expression of a suggested biomarker for oesophageal cancer, *Karyopherin alpha 2* (*Kpnα2*) [31] (Suppl. fig. 2D).

Having access to oesophageal tumour tissue and matched normal epithelial tissue from patients with oesophageal squamous cell carcinoma, we next performed real-time RT-PCR analysis using RNA isolated from frozen tissue specimens, to independently validate Oncomine and TCGA data findings in a South African subset of patients. Real-time RT-PCR analysis revealed significant downregulation of *Clock, Per1, Per2, Per3, Cry1, Cry2, Rev-erbα* and *RORα* in oesophageal cancer tissue compared to normal oesophageal epithelium counterparts (Fig. 1C). Interestingly, *Bmal1* expression was unchanged in both Oncomine and real-time RT-PCR analyses. To address possible correlations between gene expression changes, pair-wise correlation analyses were performed using the RT-PCR data (for genes which showed significantly altered expression), where Pearson correlation coefficients were determined comparing the

fold changes in cancer vs normal specimens. Strong positive correlations were identified between several circadian clock genes, where downregulation of one gene significantly correlated with downregulation of another (Suppl. table 1).

These results show that collective downregulation of multiple circadian clock genes associates with cervical and oesophageal tumour development.

Expression of circadian clock gene family members is dysregulated in transformed and cancer cell lines

Since circadian clock genes showed deregulated expression in patient tumour tissue, expression levels were next measured in cells grown in culture. The WI38 and SVWI38 cell lines are a useful pair in which to compare gene expression levels, as the SVWI38 cell line is an SV40 large T antigen (T-Ag) transformed derivative of the WI38 normal human fibroblast cells, hence any differences in gene expression observed can be attributed to the process of cellular transformation rather than heterogeneity between cell lines. As cells in long-term culture have been removed from the entraining influence of the SCN, the master clock in the brain, their circadian clock oscillators become out of phase with each other and require synchronisation for circadian clock gene expression to become rhythmic. Thus, to more accurately compare circadian clock gene expression patterns between cell lines, cells were synchronised, by treatment with the glucocorticoid analogue Dexamethasone, for 2 hours, which is known to be sufficient to synchronise the circadian clock of cultured cells, and circadian clock gene expression monitored immediately following synchronization. Interestingly, real-time RT-PCR analyses revealed significant downregulation of all the circadian clock genes in the transformed compared to normal WI38 cells (Fig. 2A), apart from *Rev-erbβ* and *RORβ* which displayed unchanged expression (Suppl. fig. 3A). *RORγ* was difficult to detect due to low levels of *RORγ* mRNA expression in tissues

outside of lymphoid and skeletal muscle origin (Human Protein Atlas). Synchronization itself did not significantly alter circadian clock gene expression patterns from that observed in unsynchronised cells, besides *Per1* expression which was upregulated after synchronization (data not shown). This is consistent with the reported effect of Dexamethasone in inducing *Per1* expression [32,33]. *Per1* expression was thus not included in subsequent analyses, as its levels were not representative of endogenous *Per1*. The downregulation of circadian clock genes in transformed cells suggests that transformation induces a global downregulation and repression of the circadian clock machinery.

Circadian clock gene expression levels were next measured in a panel of normal and cancer cell lines by real-time RT-PCR, immediately after synchronisation of cells for 2 hours with Dexamethasone. ARPE-19 normal primary epithelial cells were used as the representative normal cell line, with immortalised hTERT-RPE-1 cells representative of an immortalised cell line, and HeLa, CaSki and ME180, alongside WHCO1, WHCO5 and KYSE30, representative of cervical cancer cell lines and oesophageal cancer cell lines, respectively. *Clock*, *Bmal1*, *Cry1* and *RORα* showed significantly decreased expression in nearly all the cancer cell lines compared to normal (Fig. 2B). Expression of *Per2* was decreased in two of the three cervical cancer cell lines but increased in the oesophageal cancer cell lines. Interestingly, the negative regulator *Rev-erbα* was expressed at increased levels in the cancer cell lines compared to normal, contrary to the positive regulator *RORα* (Fig. 2B). *Cry2* and *Per3* expression was largely unchanged in the cancer cell lines compared to normal, consistent with the cervical cancer patient data, as well as expression of *Rev-erbβ* and *RORβ* (with *RORγ* again difficult to detect) (Suppl. fig. 3B). Immortalised hTERT-RPE-1 cells similarly showed reduced expression of *Clock, Bmal1, Cry1 and RORα,* with *Rev-erbα* at increased levels. Overall, these results reveal deregulation of several circadian clock genes in cancer cell lines compared to normal and suggest that the process of cell immortalization itself might be sufficient to deregulate circadian clock gene mRNA expression.

At the protein level, protein was harvested from cells immediately following synchronisation with Dexamethasone, and Clock, Cry1, Rev-erbα and RORα were found to have decreased expression levels in transformed SVI38 cells compared to normal, with Cry1 barely detected in the transformed cells (Fig. 2C). Per2, on the other hand, was present at increased levels in the transformed cells compared to normal, and a dominant upper band was present likely indicative of post-translationally modified Per2. There is extensive post-translational regulation of circadian clock genes that occurs in the circadian clock pathway, including ubiquitination, phosphorylation, glycosylation, acetylation and sumoylation, amongst others [1], and SV40 T-Ag-induced transformation appears to alter post-translational control of Per2. In the cancer cell lines, Clock, Cry1, Rev-erbα and RORα were found at decreased levels in most of the cancer cell lines compared to normal, while Bmal1 levels were largely unchanged and Per2 found at elevated levels in most of the cancer cell lines compared to normal (Fig. 2D). These results largely support the mRNA findings, with certain exceptions, and highlight the fact that mRNA and protein levels do not always correlate, as demonstrated in previous studies [34,35].

Together, these results reveal a significant downregulation or deregulation of circadian clock gene family members, particularly Clock, Cry1and RORα in transformed and cancer cell lines at the mRNA and protein levels, consistent with findings using patient tumour tissue. These differences in expression between cell lines were evident not only immediately following synchronization but also at 12 and 24 hours post-synchronisation (Suppl. fig. 4). Their altered expression in cancer cells suggests these genes might be important players in mediating cancer biology.

Circadian clock gene downregulation is associated with methylation

Previous reports describe hypermethylation of circadian clock gene promoters in breast cancer and ovarian cancer cells [36,37]. Thus, to investigate whether methylation might be contributing to circadian clock gene downregulation in cervical and oesophageal cancer cells, cells were treated with the methylation inhibitor, 5-aza-2-deoxycytidine (5aza-2-dc) and circadian clock gene expression determined. Cells were treated daily for 3 days, whereafter circadian clock gene expression was monitored by real-time RT-PCR. Results showed that circadian clock genes, *Cry1* and *RORα*, were consistently upregulated after treatment with 5aza-2dc, in all the cancer cell lines tested, and *Clock* was upregulated in two of the three cancer cell lines (Fig. 3A, B, C). *Per2* expression was increased in HeLa cells only (Fig. 3D), while *Bmal1* and Rev-*erbα* expression was unchanged in response to 5-aza-2-dc treatment (data not shown). Treatment of normal ARPE-19 cells did not result in upregulation of circadian clock genes but rather resulted in decreased expression of circadian clock genes, suggesting that the effect of methylation in downregulating circadian clock gene expression is cancer-specific (Fig. 3A-D). At the protein level, increased expression of Clock, RORα and Per2 (modified and unmodified forms) was observed in representative HeLa cells after methylation inhibition with 5-aza-2-dc (Fig. 3E). Cry1 protein levels were marginally increased but difficult to examine due to their low levels of expression in cancer cells (Fig. 3E). In contrast, ARPE19 non-cancer cells did not display increased levels of Clock, RORα or Cry1 protein after 5-aza-2-deoxycytidine treatment, and in fact levels were decreased after treatment, in line with the mRNA findings. Per2 protein, on the other hand, was present at increased levels after 5-aza-2-deoxycytidine treatment of ARPE19 cells, as were levels of its modified form, suggesting that the Per2 protein is regulated by methylation in both normal and cancer cells. The unchanged *Per2* mRNA levels in ARPE19 cells upon 5-aza-2-deoxycytidine treatment (Fig. 3D) suggest that this effect on Per2 protein levels is indirect, for example via its stabilization in response to the inhibition of methylation.

Since cancer cells displayed increased expression of *Clock, RORα, Cry1,* and *Per2* at the mRNA/protein level in response to methylation inhibition with 5-aza-2-deoxycytidine, the methylation status of these genes was next investigated in order to determine whether there was direct methylation of their promoter regions. CpG island prediction software (Methprimer) was used and CpG islands were identified in the 5' DNA regulatory sequences of *Clock, RORα, Cry1* and *Per2* genes (predominantly in the region -1000 to +1000, where the transcription start site is +1) (Suppl. fig. 5). Methylation-specific PCR was next performed, where primers were designed to bind CpG-rich sites. Two sets of primers were designed for each gene to discriminate between methylated and unmethylated DNA. Cell line genomic DNA was bisulfite converted to allow for the conversion of all unmethylated cytosines to uracil, and amplification carried out using both primer sets. CpG methylase (SssI)-treated bisulfite-converted HeLa and ME180 genomic DNA served as positive controls for the methylation-specific primers (as CpG methylase methylates all cytosines within CG dinucleotides) and PCR analysis followed by gel electrophoresis revealed that methylation-specific primers positively amplified CpG methylase-treated DNA, as expected (Fig. 3F, first two panels).

For analysis of the methylation status of each cell line, methylation-specific PCR revealed that *Clock, RORα* and *Cry1* genes were all methylated to varying extents in their 5' upstream regulatory regions in the CpG-rich regions examined (Fig. 3F). Interestingly, *Per2* was not methylated in any of the cell lines tested (Fig. 3F). While the *Cry1* gene promoter was fully methylated in all five cancer cell lines (no bands were detected using primers designed to amplify unmethylated DNA), *Clock* and *RORα* genes were found to be partially methylated, where DNA was amplified using both unmethylated and methylated primer sets. This could be due to the methylation of only one allele per gene.

To further investigate whether methylation was responsible for the decreased expression of circadian clock genes in cancer cells, it was determined whether treatment with 5-aza-2-deoxycytidine could reduce methylation of *Clock*, *RORα* and *Cry1* circadian clock gene promoters, thereby contributing to their reactivated expression in response to 5-aza-2-deoxycytidine treatment. Cells were treated with 5-aza-2-deoxycytidine for three days and DNA bisulfite converted before real-time methylation-specific PCR was performed. Positive amplification of *Clock, RORα* and *Cry1* was clearly detected in untreated cancer cells using methylation-specific primers, which decreased after treatment with varying concentrations of 5-aza-2-deoxycytidine. Methylation of *Clock, RORα* and *Cry1* gene promoters was also investigated in ARPE19 cells but it was found that ARPE19 cells displayed substantially reduced methylation of *Clock, RORα* and *Cry1* gene promoters compared to cancer cells. There were, however, low levels of promoter methylation detected in these cells, which became apparent as the number of amplification cycles increased (Fig. 3G). Interestingly, however, unlike in the cancer cells, methylation of *Clock, RORα* and *Cry1* gene promoters was not reduced upon treatment of ARPE19 cells with 5-aza-2-deoxycytidine.

Together, these results demonstrate that cancer cells lines exhibit low levels of *Clock, Cry1* and *RORα* gene expression due, at least in part, to hypermethylation of CpG islands in their promoter regions. While the Per2 promoter was not found to be methylated, the increased expression of Per2 in response to methylation inhibition could be an indirect effect, and possibly due to the regulation of Per2 expression/stability by *Clock, Cry1* and *RORα* gene family members.

Constitutive expression of Clock and Per2 and activation of Rev-erbα and RORα results in suppressed cancer cell proliferation

As cervical and oesophageal cancer patient tissue and cell lines displayed reduced circadian clock gene expression, it was next investigated whether there was a link between downregulated circadian clock gene expression and cancer biology. Circadian clock genes were overexpressed in cervical and oesophageal cancer cells, as well as in non-cancer ARPE19 cells, using circadian clock gene expression plasmids, and cell proliferation monitored using the MTT assay. HeLa, CaSki, ME180 and WHCO5 cancer cell lines all displayed significantly reduced proliferation after *Clock* and *Per2* overexpression, compared to cells transfected with the corresponding empty vector controls (Fig. 4A, B). ARPE19 cell proliferation, on the other hand, was unaffected by *Clock* or *Per2* overexpression. *Bmal1* and *Cry1* overexpression did not significantly affect cell proliferation in any of the cell lines (Fig. 4C, D). Western blot analysis confirmed successful overexpression of all circadian clock genes (Fig. 4E). Interestingly, the more slowly migrating modified form of Per2 was again observed in the Per2 overexpressing cell lysates.

To explore the effect of enhancing Rev-erbα and RORα activity on cell proliferation, cells were treated with Rev-erbα and RORα agonists, SR9011 [38] and SR1078 [39], respectively. These agonists have been reported to specifically enhance Rev-erbα and RORα receptor function. Cells were treated with agonists for 72 hours and MTT analysis revealed that treatment with both agonists resulted in significantly reduced cancer cell proliferation, in a dose-dependent manner, in all cancer cell lines, with the effects of the RORα agonist SR1078 being more potent than the Rev-erbα agonist SR9011 at equivalent concentrations (Fig. 4F, G). Interestingly, normal epithelial ARPE19 cells were significantly less affected by treatment, with SR9011 having no inhibitory effect on cell proliferation, and SR1078 only able to reduce cell proliferation at the highest concentration tested (lower concentrations of SR1078 in fact enhanced ARPE19 cell proliferation) (Fig. 4F, G). Proliferation assays performed on WI38 and SVWI38 cells treated with agonists too revealed that SR9011 was more potent at killing transformed cells compared to normal counterparts, although SR1078 was effective at killing both cell lines (Suppl. fig. 6).

Trypan blue assays verified results in representative cancer cell lines, revealing a significantly reduced number of cancer cells upon SR9011 and SR1078 treatment, and a significantly increased number of dead cells, signifying that Rev-erbα and RORα activation results in the induction of cancer cell death (Fig. 4H, I).

To corroborate the induction of cell death upon Rev-erbβ and RORα agonist treatment, Caspase-3/7 activity was measured in cancer cells after treatment with SR9011 and SR1078. Caspase-glo-3/7 activity was significantly induced in HeLa, ME180 and WHCO5 cells upon treatment with agonists, confirming the induction of apoptosis in response to Rev-erbβ and RORα activation (Fig. 4J). Increased cleavage of Parp-1 protein was also observed in cancer cells upon treatment, again confirming apoptosis as the mechanism of cell death (Fig. 4K).

Together, these results show that the overexpression/activation of specific circadian clock gene family members, *Per2, Clock, RORα* and *Rev-erbα,* acts to suppress the proliferation and viability of cancer cells, resulting in cancer cell death via apoptosis, while having a lesser effect on non-cancer cells.

Rhythmic activity of circadian clock genes in cancer cells

The functional impact of circadian clock gene downregulation in cancer cells was further investigated by measuring the circadian rhythms of cervical cancer and oesophageal cancer cells. Luminescence was measured in cervical and oesophageal cancer cells harbouring a destabilised luciferase (*dLuc*) gene under the control of the *Per2* or *Bmal1* promoter. These stable *Per2-dLuc* or *Bmal1-dLuc* cells were generated using the Tol2 transposon system [16]. Real-time monitoring of luciferase activity revealed fluctuations in *Per2-dLuc* activity in unsynchronized HeLa and WHCO5 cancer cells (Suppl. fig. 7), which

was significantly enhanced upon synchronisation with Dexamethasone, where robust rhythmic expression of *Per2-dLuc* was observed (Fig. 5A). Data was detrended and the best corresponding cosinor curve fit, whereafter the period could be calculated using the Jenkins and Watts autoperiodogram test. A period of 26.0 ± 0.83 hr and 25.9 ± 0.84 was determined for HeLa and WHCO5 cell lines, respectively, close to the intrinsic 24 hour timing of normal cells. *Bmal1-dLuc* activity showed an inverse pattern of oscillation to *Per2-dLuc* activity and was antiphase, as is expected of positive and negative circadian clock regulators (Fig. 5B). Plots of peak activity are shown in Fig. 5C.

Real-time monitoring of luciferase activity in additional cancer cell lines revealed distinct circadian oscillation of *Per2*-driven bioluminescence in all the cervical cancer (Fig. 5Di) and oesophageal cancer (Fig 5Dii) cell lines tested. Cosinor curves fitted to each dataset are shown, where the population-mean cosinor method was used (using TSA-Cosinor software). While amplitude varied between cell lines, this could be due to variability in total luminescence emitted from cells (due to different transfection efficiencies of cell lines and varying cell confluency), rather than heterogeneity between cell lines. Circadian oscillations are better compared by measuring the circadian phase and period. Interestingly, all cancer cells displayed a period of between 24 and 27 hours, and similar acrophase (peak in *Per2-dLuc* activity), except for the metastatic cervical cancer cell line, CaSki, which displayed a significantly delayed phase and increased period, compared to the non-metastatic cervical cancer, HeLa and ME180, and oesophageal cancer, WHCO5 and KYSE30 cells (Fig 5E). This is consistent with previous reports describing a delayed circadian phase and increased circadian period in metastatic cancer cell lines [40]. As a control the circadian rhythm of human osteosarcoma cells, U2OS, was analysed, as this is a widely used *in vitro* model to study properties of the mammalian circadian clock [41]. Importantly, similar circadian rhythms were observed in the cervical cancer and oesophageal cancer cells as the U2OS cells

(Fig. 5E). Together, these results reveal that despite dysregulated circadian clock gene expression, cervical cancer and oesophageal cancer cell lines maintain functional circadian oscillations. **Discussion**

This study identifies suppressed expression of circadian clock gene family members in cervical and oesophageal tumour tissue, compared to normal epithelium, as well as in cultured cervical and oesophageal cancer cell lines, compared to normal epithelial cells. Furthermore, it reveals that despite dysregulated gene expression, cervical cancer and oesophageal cancer cells display overt circadian rhythms, based on their oscillating profiles of *Per2* and *Bmal1* promoter activity after synchronization. In addition, it shows that perturbation of the circadian clock pathway, via overexpression of *Clock* and *Per2* genes, or activation of *RORα* and *Rev-erbα* using small molecules, inhibits cancer cell biology (Figure 6).

Circadian clock gene expression has been reported to be altered in various cancer types, where circadian clock genes have been reported to be downregulated in breast cancer [9], colorectal cancer [42], tongue squamous cell carcinoma [43] and gastric cancer [44], amongst others. There are multiple mechanisms by which dysregulated circadian clock gene expression may occur, for example, via the action of oncogenes or cancer/testis antigens. Relogio et al. (2014) showed how Ras perturbation can disrupt the circadian clock and revealed differential expression of core clock genes in normal and Ras-transformed cells [40], while Michael et al. (2015) showed how the cancer/testis antigen *Pasd1* represses Bmal1:Clock activity in cancer cells [45]. Hypermethylation of the promoter regions of circadian clock genes has also been described, acting to downregulate circadian clock gene expression in breast cancer tissue [36] and ovarian cancer cells [46]. Our study shows decreased expression of core circadian clock genes in cervical and oesophageal cancer cells, and reveals that methylation plays a direct role in mediating downregulated *Clock*, *Cry1* and *RORα* gene expression, and indirectly affects *Per2* expression levels. The role of other

factors such as oncogenes and cancer/testis antigens in further controlling circadian clock gene expression remains to be determined.

It was noted in our study that the mRNA and protein profiles of circadian clock genes did not always correlate. Shu et al (2004) describe how circadian clock gene oscillations are controlled by four-step-expression, where transcription, translation, degradation of mRNA, and degradation of protein are all vital in controlling gene expression [47]. It is possible that in the cancer cell lines in our study, differing protein/mRNA half-life in different cell lines may lead to the lack of correlation between mRNA and protein. Furthermore, a modified, more slowly migrating form of Per2 protein was observed in transformed SVWI38 cells (Fig. 2C), HeLa and ARPE19 cells treated with methylation inhibitor 5-aza-2-deoxycytidine (Fig. 3E), and in cells in which Per2 was overexpressed (Fig. 4E). Miyazaki et al. (2004) reported that the size of Per2 fluctuates after synchronization of WI38 cells (it increases in size up to approximately 200 kDa: the size of the modified Per2 protein in our study) and showed that this is due to phosphorylation of Per2 by CKI (casein kinase I) proteins [48]. It has also been reported by Camacho et al (2001) that CKI proteins can phosphorylate overexpressed Per1 and Per2 *in vitro* and induce an increase in the apparent molecular size of Per proteins [49]. Future work will be required to investigate why increased phosphorylation of Per2 might be occurring under the various cellular conditions observed.

Chang and Lai (2019) recently showed that circadian clock genes that confer tumour suppressing effects in one cancer type can play an opposing role and exhibit tumour-promoting effects in another cancer type [13]. We show that in cervical and oesophageal tumour cells *Per2, Clock, RORα* and *Rev-erbα* display tumour-inhibiting properties, as their overexpression/activation (in cells displaying low levels of expression) results in reduced cell proliferation. Furthermore, we show that while cancer cells undergo

cell death upon activation of *RORα* and *Rev-erbα*, normal cells respond differently. ARPE19 and WI38 non-cancer cells are less sensitive to SR9011 compared to cancer and transformed cells, where concentrations that result in cancer cell death do not inhibit ARPE19 or WI38 cell proliferation. In addition, APRE19 cell proliferation is only inhibited at SR1078 concentrations of >30 μM, although WI38 cells are sensitive to lower concentrations of SR1078. These results suggest that *Per2, Clock, RORα* and *Rev-erbα* circadian clock genes might have potential as druggable targets, whereby their activation could have therapeutic potential. Rev-erbα agonists have been suggested to be potential treatment options for different types of cancer [50]. The activation of Rev-erbα has been proven advantageous in that it appears to be non-damaging to healthy tissue, and can act to rid the tumour of not only actively proliferating cells, but also oncogene-induced senescent cells, which play a role in mediating chemotherapy resistance and relapse [50]. It has been proposed that Rev-erbα activation suppresses expression of Cyclin A in breast cancer cells, contributing to cell cycle arrest [51]. The activation of RORα has been shown to induce p53 expression and activate cell death in HepG2 cells [39]. Our results support the use of Rev-erbα and RORα agonists, SR9011 and SR1078, against cervical and oesophageal cancers. Further work investigating the use of these agonists in treating these types of cancer is required. Particularly, further studies are needed to address whether the overexpression/activation of circadian clock components leads to the observed anti-tumoural effects via interfering with the circadian rhythm of cancer cells, or via alternate pathways.

Our study also examined the circadian oscillatory profiles of cervical and oesophageal cancer cells. Literature suggests that the circadian rhythm is often suppressed in cancer cells. Breast cancer cells have been shown to display arrhythmic patterns of circadian clock gene expression, and while serum shock can induce oscillation of some circadian clock genes, the amplitude is greatly reduced compared to normal breast epithelial cells [52–55]. More recently, however, Lellupitiyage et al. (2019) showed that low

malignancy MCF7 cells do display circadian oscillations of *Per2* and *Bmal1*, while high-grade MDA-MB-231 cells do not [56]. In tumour tissue *in vivo*, it has been previously shown that Glasgow osteosarcoma and pancreatic adenocarcinoma tissues display absent, or very weak rhythmic profiles of circadian clock genes [7,57]. Interestingly, Relogio et al. (2014) describe how colon cancer cell lines show a rich variety of circadian phenotypes, where some showed strong and others weak to no-oscillation phenotypes (these authors classify a strong oscillator as a cell line with a clear circadian period and amplitude variation of at least 20 %) [40]. Moreover, they identified a list of genes able to discriminate between weak and strong oscillator cell lines by transcriptome analysis, and the roles of these genes in both circadian clock and oncogenic pathways suggests these pathways are strongly connected. Our results show that the cervical and oesophageal cancer cells examined display strong oscillating phenotypes, despite deregulated circadian clock gene expression. There was little difference in the period and acrophase described in the different cell lines, besides the CaSki metastatic cancer cell line having a significantly increased period and delayed phase compared to the other cells. Together, these findings reinforce that cancer cells can maintain rhythmic circadian profiles and suggests that these rhythmic profiles might be contributing to cancer biology.

It has been shown that the circadian rhythm of clock genes becomes markedly impaired in senescent or "aging" cells, and that this can be reversed by telomerase reconstitution [58]. As cancer cells display increased telomerase activity, this could in part explain the overt circadian rhythms observed in the cancer cell lines used in our study. Interestingly, it has also been shown that telomerase mRNA expression and activity exhibits endogenous circadian rhythmicity and is under the control of the Clock-Bmal1 heterodimer [59], revealing a feedback mechanism between telomerase and the circadian clock.

In conclusion, the disruption of circadian clock components in cancer, or “circadian reprogramming” can be a critical player in tumourigenesis, while maintenance of circadian rhythms might also act to uphold cancer-related processes. Chang and Lai (2019) demonstrate that circadian reprogramming of tumour genomes plays an important role in influencing disease progression and patient outcomes [13]. Ongoing efforts at investigating the circadian clock in cancer development are needed.

References

1. Ko, C. H. & Takahashi, J. S. Molecular components of the mammalian circadian clock. *Human Molecular Genetics* **15**, (2006).

2. Reppert, S. M. & Weaver, D. R. Coordination of circadian timing in mammals. *Nature* **418**, 935–941 (2002).

3. Zhang, R., Lahens, N. F., Ballance, H. I., Hughes, M. E. & Hogenesch, J. B. A circadian gene expression atlas in mammals: Implications for biology and medicine. *Proc. Natl. Acad. Sci.* **111**, 16219–16224 (2014).

4. Straif, K. *et al.* Carcinogenicity of shift-work, painting, and fire-fighting. *The Lancet Oncology* **8**, 1065–1066 (2007).

5. Sulli, G., Manoogian, E. N. C., Taub, P. R. & Panda, S. Training the Circadian Clock, Clocking the Drugs, and Drugging the Clock to Prevent, Manage, and Treat Chronic Diseases. *Trends in Pharmacological Sciences* **39**, 812–827 (2018).

6. Papagiannakopoulos, T. *et al.* Circadian Rhythm Disruption Promotes Lung Tumorigenesis. *Cell Metab.* **24**, 324–331 (2016).

7. Li, X. M. *et al.* Cancer inhibition through circadian reprogramming of tumor transcriptome with meal timing. *Cancer Res* **70**, 3351–3360 (2010).

8. Davis, K., Roden, L. C., Leaner, V. D. & van der Watt, P. J. The tumour suppressing role of the circadian clock. *IUBMB Life* (2019). doi:10.1002/iub.2005

9. Cadenas, C. *et al.* Loss of circadian clock gene expression is associated with tumor progression in breast cancer. *Cell Cycle* **13**, 3282–3291 (2014).

10. Hsu, C. M., Lin, S. F., Lu, C. T., Lin, P. M. & Yang, M. Y. Altered expression of circadian clock genes in head and neck squamous cell carcinoma. *Tumor Biol.* (2012). doi:10.1007/s13277-011-0258-2

11. He, Q. Y. *et al.* Prognostic significance of downregulated BMAL1 and upregulated Ki-67 proteins in nasopharyngeal carcinoma. *Chronobiol. Int.* (2018). doi:10.1080/07420528.2017.1406494

12. Xiong, H. *et al.* Loss of the clock gene PER2 is associated with cancer development and altered expression of important tumor-related genes in oral cancer. *Int. J. Oncol.* (2018). doi:10.3892/ijo.2017.4180

13. Chang, W. H. & Lai, A. G. Timing gone awry: distinct tumour suppressive and oncogenic roles of the circadian clock and crosstalk with hypoxia signalling in diverse malignancies. *J. Transl. Med.* (2019). doi:10.1186/s12967-019-1880-9

14. Altman, B. J. *et al.* MYC Disrupts the Circadian Clock and Metabolism in Cancer Cells. *Cell Metab.* **22**, 1009–1019 (2015).

15. Bray, F. *et al.* Global cancer statistics 2018: GLOBOCAN estimates of incidence and mortality worldwide for 36 cancers in 185 countries. *CA. Cancer J. Clin.* (2018). doi:10.3322/caac.21492

16. Yagita, K., Yamanaka, I., Emoto, N., Kawakami, K. & Shimada, S. Real-time monitoring of circadian clock oscillations in primary cultures of mammalian cells using Tol2 transposon-mediated gene transfer strategy. *BMC Biotechnol.* (2010). doi:10.1186/1472-6750-10-3

17. Sato, T. K. *et al.* Feedback repression is required for mammalian circadian clock function. *Nat. Genet.* (2006). doi:10.1038/ng1745

18. Vielhaber, E., Eide, E., Rivers, A., Gao, Z.-H. & Virshup, D. M. Nuclear Entry of the Circadian Regulator mPER1 Is Controlled by Mammalian Casein Kinase I. *Mol. Cell. Biol.* (2000).

19. Huang, N. *et al.* Crystal structure of the heterodimeric CLOCK:BMAL1 transcriptional activator

complex. *Science (80-.).* (2012). doi:10.1126/science.1222804

20. Lee, Y. *et al.* Coactivation of the CLOCK-BMAL1 complex by CBP mediates resetting of the circadian clock. *J. Cell Sci.* (2010). doi:10.1242/jcs.070300

21. Livak, K. J. & Schmittgen, T. D. Analysis of relative gene expression data using real-time quantitative PCR and the 2-ΔΔCT method. *Methods* (2001). doi:10.1006/meth.2001.1262

22. Davidović, R. S., Božović, A. M., Mandušić, V. L. & Krajnović, M. M. Methylation-specific PCR: Four steps in primer design. *Central European Journal of Biology* (2014). doi:10.2478/s11535-014-0324-z

23. Van Der Watt, P. J. *et al.* The karyopherin proteins, Crm1 and Karyopherin β1, are overexpressed in cervical cancer and are critical for cancer cell survival and proliferation. *Int. J. Cancer* (2009). doi:10.1002/ijc.24146

24. Ward, M. C., Van Der Watt, P. J., Tzoneva, G. & Leaner, V. D. Deregulated LAP2α expression in cervical cancer associates with aberrant E2F and p53 activities. *IUBMB Life* (2011). doi:10.1002/iub.528

25. Rhodes, D. R. *et al.* Oncomine 3.0: genes, pathways, and networks in a collection of 18,000 cancer gene expression profiles. *Neoplasia* (2007).

26. Zhai, Y. *et al.* Gene expression analysis of preinvasive and invasive cervical squamous cell carcinomas identifies HOXC10 as a key mediator of invasion. *Cancer Res.* (2007). doi:10.1158/0008-5472.CAN-07-2056

27. Scotto, L. *et al.* Identification of copy number gain and overexpressed genes on chromosome arm 20q by an integrative genomic approach in cervical cancer: Potential role in progression. *Genes Chromosom. Cancer* (2008). doi:10.1002/gcc.20577

28. Wang, Q. *et al.* Data Descriptor: Unifying cancer and normal RNA sequencing data from different sources. *Sci. Data* (2018). doi:10.1038/sdata.2018.61

29. Hu, N. *et al.* Genome wide analysis of DNA copy number neutral loss of heterozygosity (CNNLOH) and its relation to gene expression in esophageal squamous cell carcinoma. *BMC Genomics* (2010). doi:10.1186/1471-2164-11-576

30. Su, H. *et al.* Global gene expression profiling and validation in esophageal squamous cell carcinoma and its association with clinical phenotypes. *Clin. Cancer Res.* (2011). doi:10.1158/1078-0432.CCR-10-2724

31. Ma, S. & Zhao, X. KPNA2 is a promising biomarker candidate for esophageal squamous cell carcinoma and correlates with cell proliferation. *Oncol. Rep.* **32**, 1631–1637 (2014).

32. Balsalobre, A., Marcacci, L. & Schibler, U. Multiple signaling pathways elicit circadian gene expression in cultured Rat-1 fibroblasts. *Curr. Biol.* (2000). doi:10.1016/S0960-9822(00)00758-2

33. Balsalobre, A. *et al.* Resetting of circadian time in peripheral tissues by glucocorticoid signaling. *Science (80-.).* (2000). doi:10.1126/science.289.5488.2344

34. Robles, M. S., Cox, J. & Mann, M. In-Vivo Quantitative Proteomics Reveals a Key Contribution of Post-Transcriptional Mechanisms to the Circadian Regulation of Liver Metabolism. *PLoS Genet.* (2014). doi:10.1371/journal.pgen.1004047

35. Ghazalpour, A. *et al.* Comparative analysis of proteome and transcriptome variation in mouse. *PLoS Genet.* (2011). doi:10.1371/journal.pgen.1001393

36. Kuo, S.-J. *et al.* Disturbance of circadian gene expression in breast cancer. *Virchows Arch.* **454**, 467–474 (2009).

37. Yeh, C.-M. *et al.* Epigenetic silencing of ARNTL, a circadian gene and potential tumor suppressor

in ovarian cancer. *Int. J. Oncol.* (2014). doi:10.3892/ijo.2014.2627

38. Solt, L. A. *et al.* Regulation of circadian behaviour and metabolism by synthetic REV-ERB agonists. *Nature* (2012). doi:10.1038/nature11030

39. Wang, Y., Solt, L. A., Kojetin, D. J. & Burris, T. P. Regulation of p53 stability and apoptosis by a ROR agonist. *PLoS One* (2012). doi:10.1371/journal.pone.0034921

40. Relógio, A. *et al.* Ras-Mediated Deregulation of the Circadian Clock in Cancer. *PLoS Genet.* **10**, (2014).

41. Zhang, E. E. *et al.* A Genome-wide RNAi Screen for Modifiers of the Circadian Clock in Human Cells. *Cell* (2009). doi:10.1016/j.cell.2009.08.031

42. Mazzoccoli, G. *et al.* Clock Gene Expression Levels and Relationship With Clinical and Pathological Features in Colorectal Cancer Patients. *Chronobiol. Int.* **28**, 841–851 (2011).

43. Tang, Q. *et al.* Circadian clock gene Bmal1 inhibits tumorigenesis and increases paclitaxel sensitivity in tongue squamous cell carcinoma. *Cancer Res.* **77**, 532–544 (2017).

44. Zhao, H. *et al.* Prognostic relevance of Period1 (Per1) and Period2 (Per2) expression in human gastric cancer. *Int. J. Clin. Exp. Pathol.* (2014).

45. Michael, A. K. *et al.* Cancer/Testis Antigen PASD1 Silences the Circadian Clock. *Mol. Cell* **58**, 743–754 (2014).

46. Yeh, C. M. *et al.* Epigenetic silencing of ARNTL, a circadian gene and potential tumor suppressor in ovarian cancer. *Int. J. Oncol.* (2014). doi:10.3892/ijo.2014.2627

47. Shu, Y. & Hong-Hui, L. Transcription, translation, degradation, and circadian clock. *Biochemical and Biophysical Research Communications* (2004). doi:10.1016/j.bbrc.2004.06.093

48. MIYAZAKI, K. *et al.* Phosphorylation of clock protein PER1 regulates its circadian degradation in

normal human fibroblasts. *Biochem. J.* (2004). doi:10.1042/bj20031308

49. Camacho, F. *et al.* Human casein kinase Iδ phosphorylation of human circadian clock proteins period 1 and 2. *FEBS Lett.* (2001). doi:10.1016/S0014-5793(00)02434-0

50. Sulli, G. *et al.* Pharmacological activation of REV-ERBs is lethal in cancer and oncogene-induced senescence. *Nature* **553**, 351–355 (2018).

51. Wang, Y., Kojetin, D. & Burris, T. P. Anti-proliferative actions of a synthetic REV-ERBα/β agonist in breast cancer cells. *Biochem. Pharmacol.* (2015). doi:10.1016/j.bcp.2015.06.010

52. Xiang, S. *et al.* Oscillation of clock and clock controlled genes induced by serum shock in human breast epithelial and breast cancer cells: Regulation by melatonin. *Breast Cancer Basic Clin. Res.* **6**, 137–150 (2012).

53. Chacolla-Huaringa, R., Moreno-Cuevas, J., Trevino, V. & Scott, S. P. Entrainment of breast cell lines results in rhythmic fluctuations of microRNAs. *Int. J. Mol. Sci.* **18**, (2017).

54. Rossetti, S., Esposito, J., Corlazzoli, F., Gregorski, A. & Sacchi, N. Entrainment of breast (cancer) epithelial cells detects distinct circadian oscillation patterns for clock and hormone receptor genes. *Cell Cycle* **11**, 350–360 (2012).

55. Gutiérrez-Monreal, M. A., Treviño, V., Moreno-Cuevas, J. E. & Scott, S. P. Identification of circadian-related gene expression profiles in entrained breast cancer cell lines. *Chronobiol. Int.* **33**, 392–405 (2016).

56. Lellupitiyage Don, S. S. *et al.* Circadian oscillations persist in low malignancy breast cancer cells. *Cell Cycle* (2019). doi:10.1080/15384101.2019.1648957

57. Iurisci, I. *et al.* Improved tumor control through circadian clock induction by Seliciclib, a cyclin-dependent kinase inhibitor. *Cancer Res* **66**, (2006).

58. Qu, Y. *et al.* Telomerase reconstitution contributes to resetting of circadian rhythm in fibroblasts. *Mol. Cell. Biochem.* (2008). doi:10.1007/s11010-008-9736-2

59. Chen, W. D. *et al.* The circadian rhythm controls telomeres and telomerase activity. *Biochem. Biophys. Res. Commun.* (2014). doi:10.1016/j.bbrc.2014.07.138

Figure legends

Figure 1. Expression of circadian clock genes in patient tumour tissue. A. Levels of circadian clock gene expression in normal and cervical cancer and/or HSIL tissue specimens, based on Oncomine™ analysis, using data obtained from (i) Scotto et al. (2008) (20 normal squamous epithelial samples and 20 primary tumours) and (ii) Zhai et al. (2007) (10 normal cervix samples, 7 HSILs and 21 invasive cervical SCCs). B. Levels of circadian clock gene expression in oesophageal cancer and matched normal tissue specimens, based on Oncomine™ analysis, using data obtained from (i) Hu et al. (2010) (n = 17) and (ii) Su et al. (2011) (n = 53). C. Real-time RT-PCR analysis showing circadian clock gene expression levels in oesophageal cancer tissue and matched normal oesophageal epithelium from South African OSCC patients (n = 24). *$p<0.05$.

Figure 2. Expression of circadian clock genes in cultured cell lines. A. Real-time RT-PCR analysis showing circadian clock gene expression levels in normal WI38 cells and matched transformed SVWI38 cells, after synchronisation. B. Real-time RT-PCR analysis showing circadian clock gene expression levels in normal ARPE19 epithelial cells, immortalized hTERT-RPE-1 epithelial cells and cervical cancer (HeLa, CaSki, ME180) and oesophageal cancer (WHCO1, WHCO5, KYSE30) cells (*$p<0.05$). C. Western blot analysis showing circadian clock protein levels in WI38 and SVWI38 cells. p38 was used as a control for protein loading. D. Western blot analysis showing circadian clock protein levels in ARPE19, hTERT-RPE-1 and cancer cell lines. Representative Western blots are shown of experiments performed at least two independent times.

Figure 3. Methylation analysis of circadian clock genes in cancer and non-cancer cells. A-D. Cervical cancer (HeLa, CaSki, ME180) and normal epithelial (ARPE19) cells were treated with 2.5, 5 or 10 µM 5-aza-2-deoxycytidine (5-aza-2-dc) for 72 hours and gene expression monitored by real-time RT-PCR. Experiments were performed in triplicate and results are shown as the mean ± SEM (*p<0.05). E. Western blot analysis showing protein levels of circadian clock genes after methylation inhibition in HeLa cells and ARPE19 cells with 5-aza-2-dc for 72 hours. F. Methylation-specific PCR analysis of *Clock, RORα, Cry1* and *Per2* genes. DNA was bisulfite-modified, PCR amplified and electrophoresed on 1.5 % agarose gels. SssI-treated DNA (bisulfite-converted) was used as a positive control for methylation-specific primers. U and M indicate methylation-specific PCR using unmethylation-specific and methylation-specific primer sets, respectively. G. Real-time methylation-specific PCR analysis of *Clock*, *RORα* and *Cry1* genes after treatment of cells with 5-aza-2-deoxycytidine for 72 hours. C_T values reflect the number of cycles required for the fluorescent signal to cross a threshold, where ut denotes undetected fluorescent signal.

Figure 4. Effect of circadian clock gene overexpression/activation on cell proliferation. A-D. Cell proliferation was measured 96 hours after circadian clock gene overexpression using the MTT assay. E. Western blot analysis showing protein overexpression with the respective circadian clock gene overexpression constructs. p38 was used as a control for protein loading. F. Cell proliferation after treatment of cells with Rev-erbα and RORα agonists, SR9011 and SR1078, for 72 hours, measured using the MTT assay. H, I. Number of live and dead cells after treatment of ME180 (i) and WHCO5 (ii) cells with SR9011 (H) and SR1078 (I) for 72 hours, measured using the trypan blue assay. J. Caspase-3/7 activity measured in cancer cells after treatment with SR9011 or SR1078 for 72 hours. Experiments were performed in triplicate and results are shown as the mean ± SEM (* denotes significance relative to untreated cells; *p<0.05). K. Western blots analysis showing uncleaved and cleaved Parp-1 protein levels

in SR9011- or SR1078-treated cancer cells. p38 was used as a protein loading control. Cleaved Parp-1 was quantified using Image J and expressed relative to uncleaved Parp-1 and p38.

Figure 5. Circadian oscillations of cancer cells. A. Real-time bioluminescence monitoring showing oscillating *Per2-dLuc* activity in synchronized HeLa (i) and WHCO5 (ii) cells over time. B. Real-time bioluminescence monitoring showing oscillating *Bmal1-dLuc* activity in synchronized HeLa (i) and WHCO5 (ii) cells over time. C. Plots showing peak *Per2-dLuc* and *Bmal1-dLuc* activity in HeLa (i) and WHCO5 (ii) cells. D. (i) Oscillating profiles of *Per2-dLuc* activity in HeLa (blue), CaSki (orange) and ME180 (red) cervical cancer cells. Cosinor plots were generated using TSA-Cosinor software. (ii) Oscillating profiles of *Per2-dLuc* activity in WHCO5 (blue) and KYSE30 (red) oesophageal cancer cells over time. E. Plots showing acrophase of *Per2-dLuc* activity (i) and period values (ii) obtained from analysis of circadian oscillations of different cell lines, using TSA-Cosinor software. Data shown are averaged across at least three independent experiments with four technical repeats in each; mean ± SEM are shown (*$p<0.05$).

Figure 6. Summary model. Under normal cellular conditions, the Clock/Bmal1 heterodimer binds E-boxes present in the promoter regions of core clock-controlled genes (CCGs), including *Per*, *Cry*, *ROR* and *Rev-erb*, activating gene expression. Once translated, Per and Cry proteins dimerise and inhibit Clock/Bmal1 activity, repressing their own transcription. ROR and Rev-erb activate and inhibit expression of *Bmal1*, respectively. The result is oscillating patterns of circadian clock gene promoter activity. In the cancer state, *Clock*, *Cry1* and *RORα* promoters are hypermethylated, repressing *Clock*, *Cry1* and *RORα* gene mRNA and protein expression, and impacting overall circadian clock gene mRNA expression levels, although oscillating promoter activity patterns are maintained. Disruption of the

circadian clock using *ROR* and *Rev-erb* agonists, SR1078 and SR9011, or overexpression of *Per* and *Clock* genes, leads to cancer cell death, suggesting perturbation of the circadian clock pathway could be exploited as an anti-cancer strategy.

Figure 1

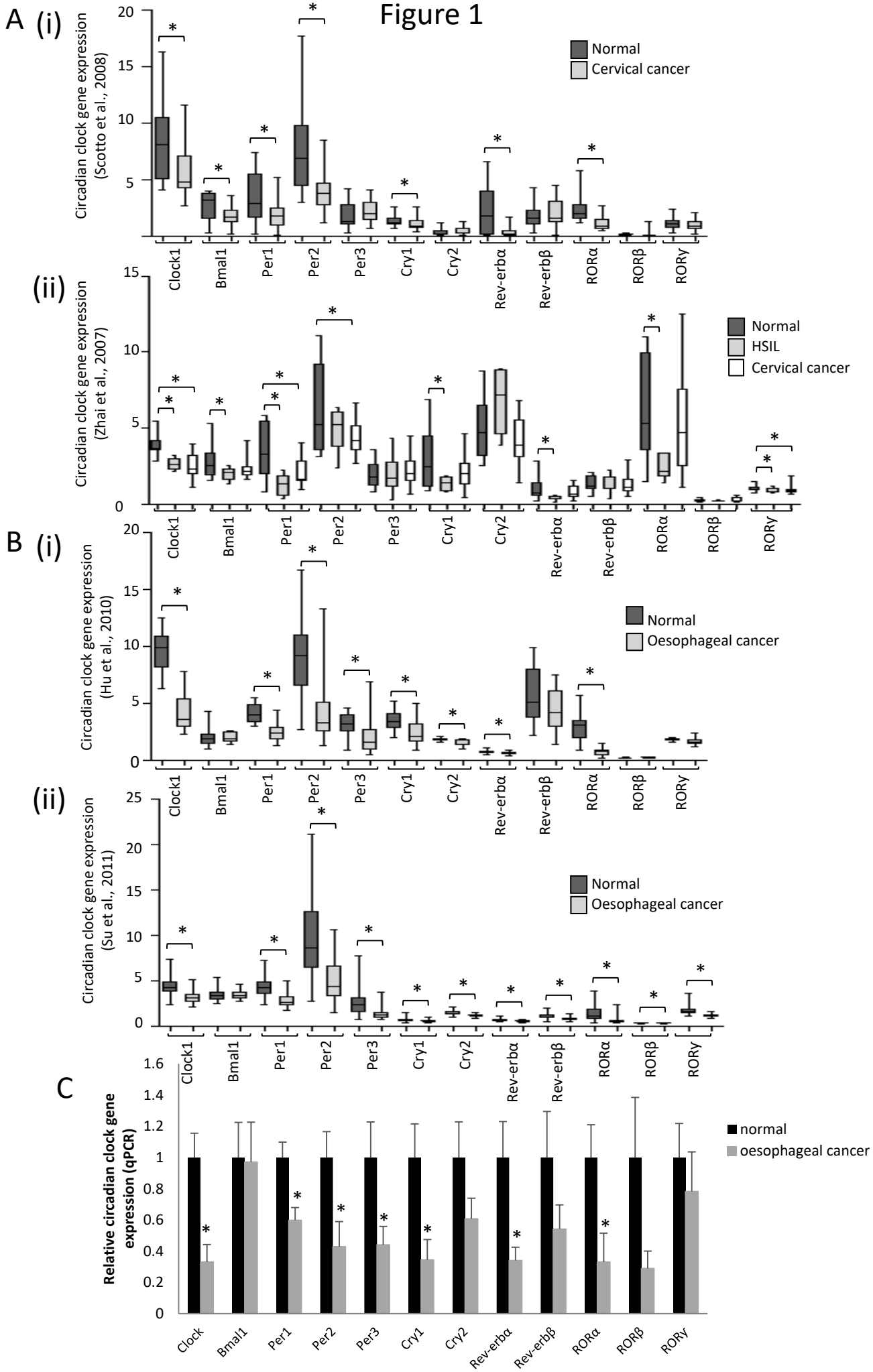
A (i)
Circadian clock gene expression (Scotto et al., 2008)
Normal
Cervical cancer
Clock1
Bmal1
Per1
Per2
Per3
Cry1
Cry2
Rev-erbα
Rev-erbβ
RORα
RORβ
RORγ
(ii)
Circadian clock gene expression (Zhai et al., 2007)
Normal
HSIL
Cervical cancer
B (i)
Circadian clock gene expression (Hu et al., 2010)
Normal
Oesophageal cancer
(ii)
Circadian clock gene expression (Su et al., 2011)
Normal
Oesophageal cancer
C
Relative circadian clock gene expression (qPCR)
normal
oesophageal cancer
Clock
Bmal1
Per1
Per2
Per3
Cry1
Cry2
Rev-erbα
Rev-erbβ
RORα
RORβ
RORγ

Figure 2

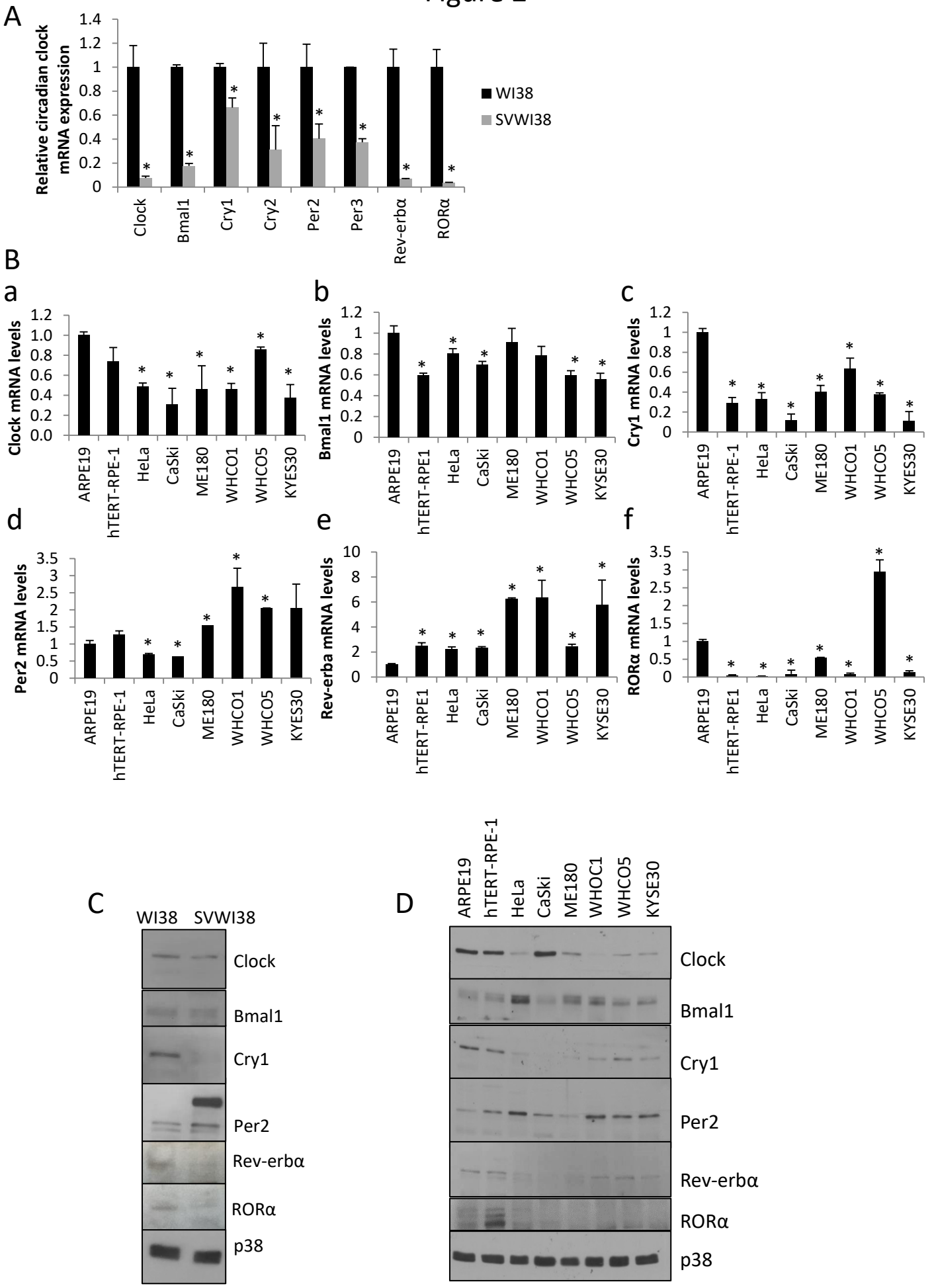
A
Relative circadian clock mRNA expression
WI38
SVWI38
Clock
Bmal1
Cry1
Cry2
Per2
Per3
Rev-erbα
RORα
B
a
Clock mRNA levels
b
Bmal1 mRNA levels
c
Cry1 mRNA levels
d
Per2 mRNA levels
e
Rev-erba mRNA levels
f
RORα mRNA levels
ARPE19
hTERT-RPE-1
HeLa
CaSki
ME180
WHCO1
WHCO5
KYSE30
C
WI38
SVWI38
Clock
Bmal1
Cry1
Per2
Rev-erbα
RORα
p38
D
ARPE19
hTERT-RPE-1
HeLa
CaSki
ME180
WHOC1
WHCO5
KYSE30
Clock
Bmal1
Cry1
Per2
Rev-erbα
RORα
p38

Figure 3

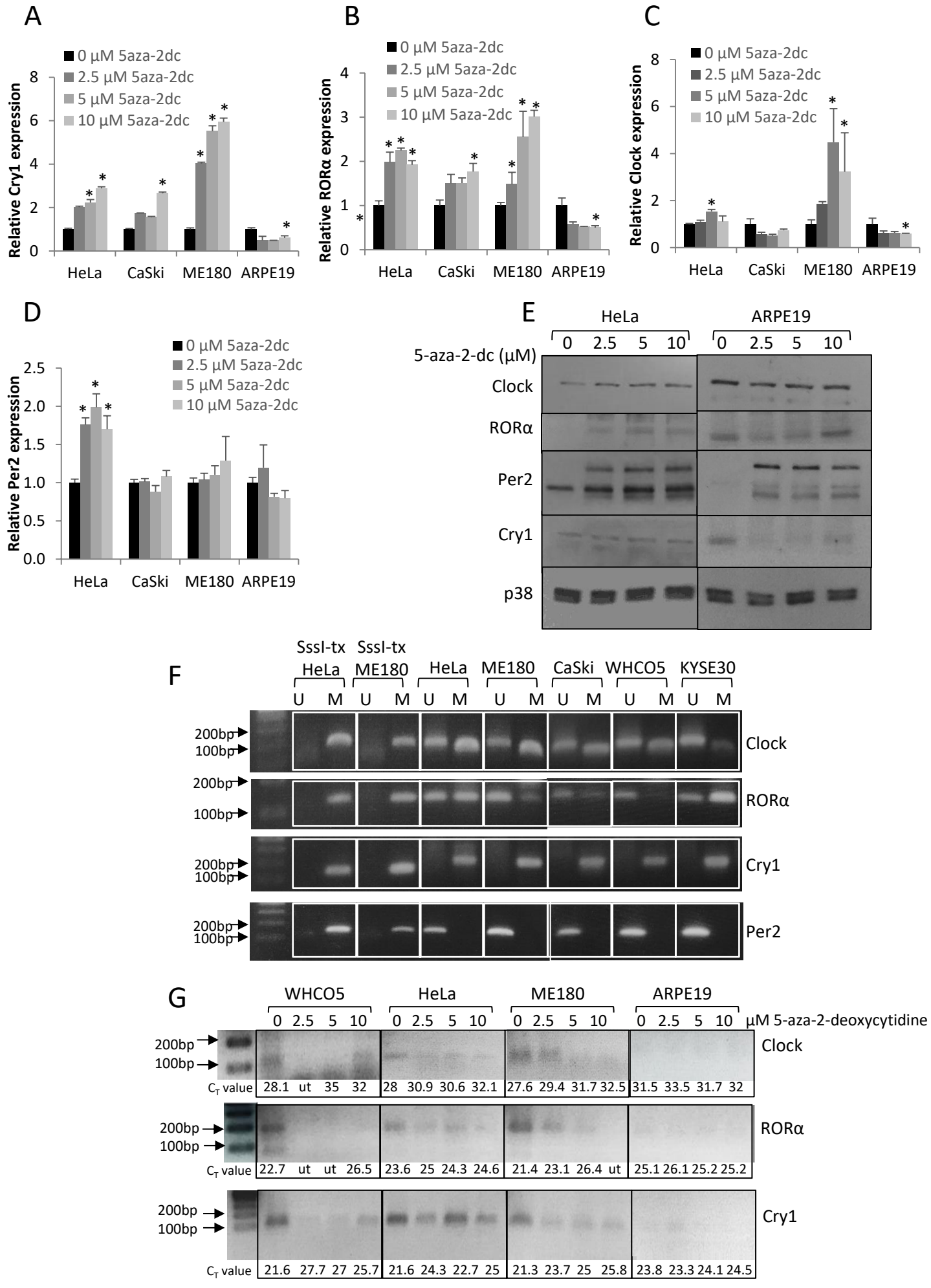
A
0 µM 5aza-2dc
2.5 µM 5aza-2dc
5 µM 5aza-2dc
10 µM 5aza-2dc
Relative Cry1 expression
HeLa
CaSki
ME180
ARPE19
B
Relative RORα expression
C
Relative Clock expression
D
Relative Per2 expression
E
HeLa
ARPE19
5-aza-2-dc (µM)
Clock
RORα
Per2
Cry1
p38
F
SssI-tx HeLa
SssI-tx ME180
HeLa
ME180
CaSki
WHCO5
KYSE30
U
M
200bp
100bp
Clock
RORα
Cry1
Per2
G
WHCO5
HeLa
ME180
ARPE19
µM 5-aza-2-deoxycytidine
200bp
100bp
Clock
C_T value
28.1 ut 35 32
28 30.9 30.6 32.1
27.6 29.4 31.7 32.5
31.5 33.5 31.7 32
RORα
22.7 ut ut 26.5
23.6 25 24.3 24.6
21.4 23.1 26.4 ut
25.1 26.1 25.2 25.2
Cry1
21.6 27.7 27 25.7
21.6 24.3 22.7 25
21.3 23.7 25 25.8
23.8 23.3 24.1 24.5

Figure 4

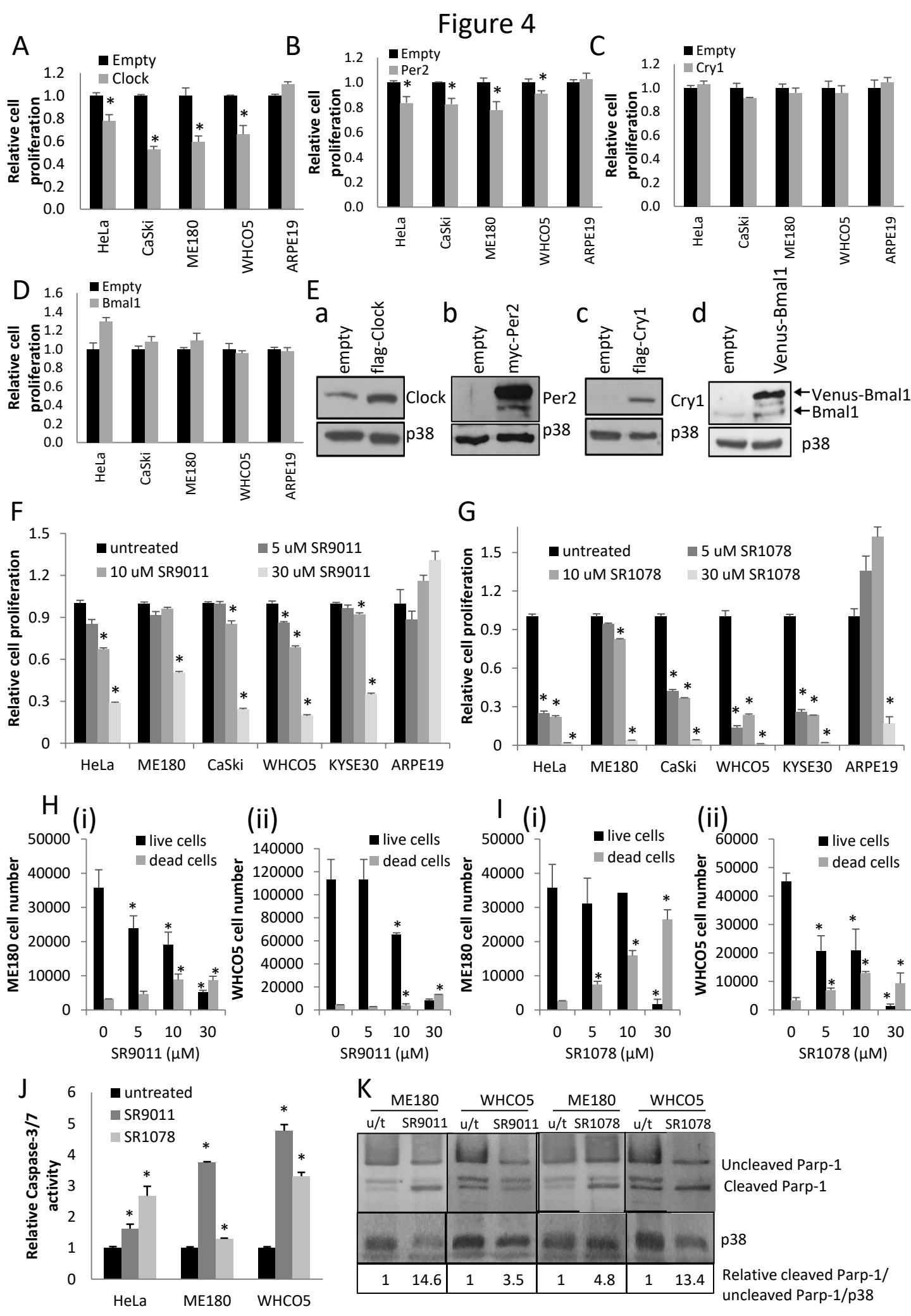
A
Empty
Clock
Relative cell proliferation
HeLa
CaSki
ME180
WHCO5
ARPE19
B
Empty
Per2
C
Empty
Cry1
D
Empty
Bmal1
E
a
empty
flag-Clock
Clock
p38
b
empty
myc-Per2
Per2
c
empty
flag-Cry1
Cry1
d
empty
Venus-Bmal1
Venus-Bmal1
Bmal1
F
untreated
5 uM SR9011
10 uM SR9011
30 uM SR9011
KYSE30
G
untreated
5 uM SR1078
10 uM SR1078
30 uM SR1078
H
(i)
(ii)
live cells
dead cells
ME180 cell number
WHCO5 cell number
SR9011 (μM)
I
SR1078 (μM)
J
untreated
SR9011
SR1078
Relative Caspase-3/7 activity
K
ME180
WHCO5
u/t
SR9011
SR1078
Uncleaved Parp-1
Cleaved Parp-1
p38
1
14.6
3.5
4.8
13.4
Relative cleaved Parp-1/ uncleaved Parp-1/p38

Figure 5

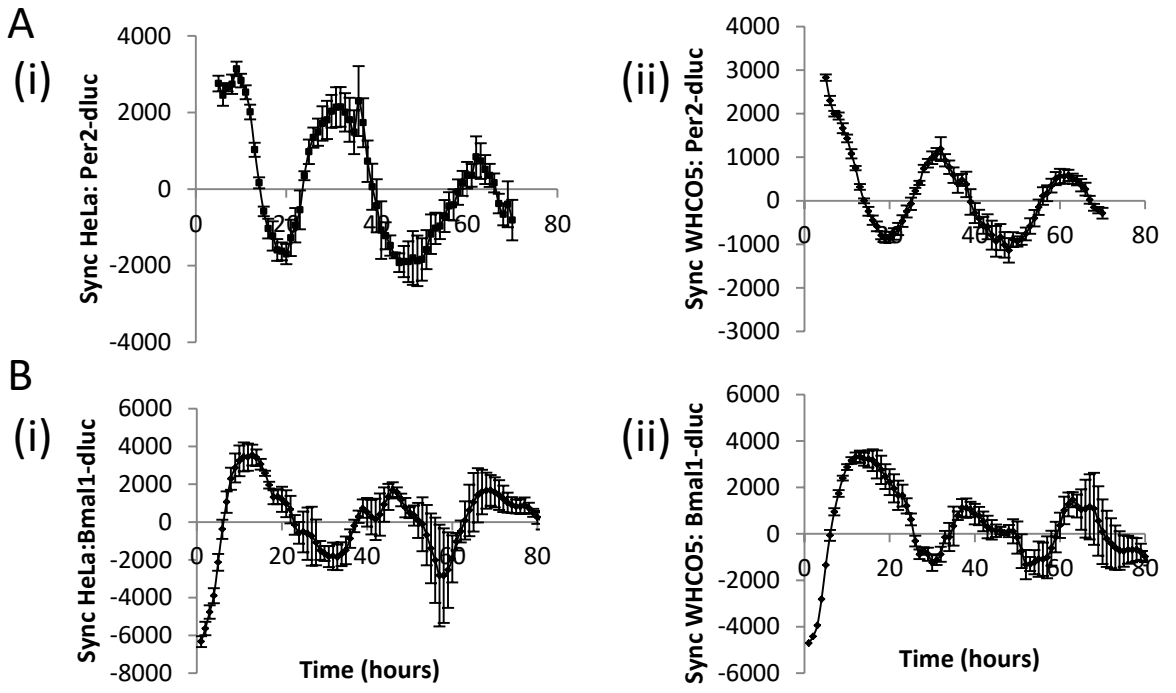
A
(i)
Sync HeLa: Per2-dluc
(ii)
Sync WHCO5: Per2-dluc
B
(i)
Sync HeLa:Bmal1-dluc
(ii)
Sync WHCO5: Bmal1-dluc
Time (hours)

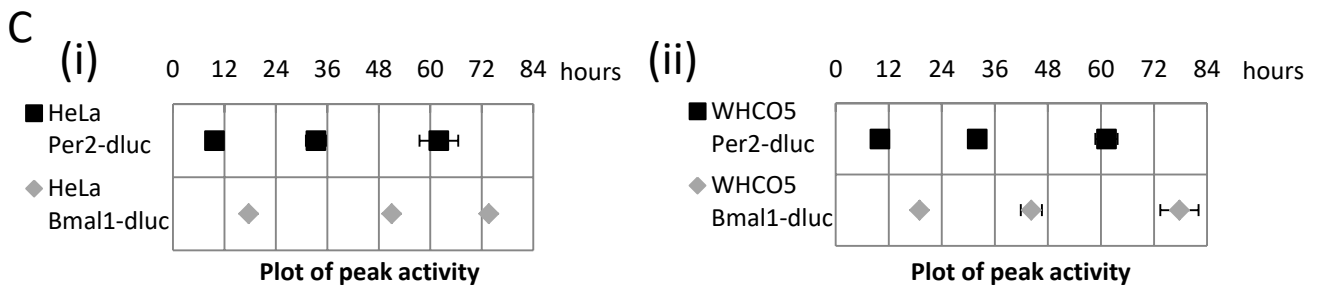
C
(i)
0 12 24 36 48 60 72 84 hours
HeLa Per2-dluc
HeLa Bmal1-dluc
Plot of peak activity
(ii)
WHCO5 Per2-dluc
WHCO5 Bmal1-dluc
Plot of peak activity

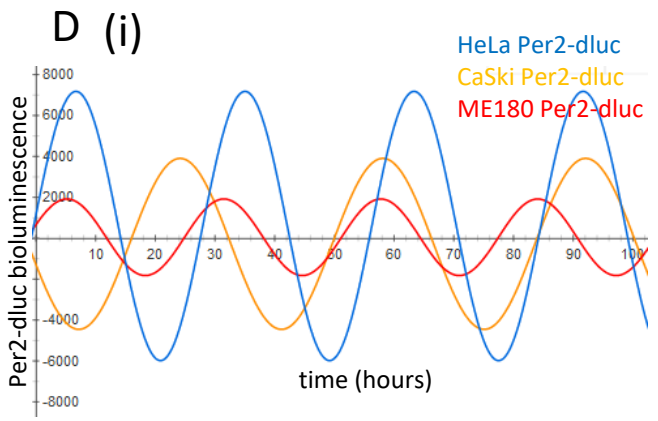
D
(i)
HeLa Per2-dluc
CaSki Per2-dluc
ME180 Per2-dluc
Per2-dluc bioluminescence
time (hours)

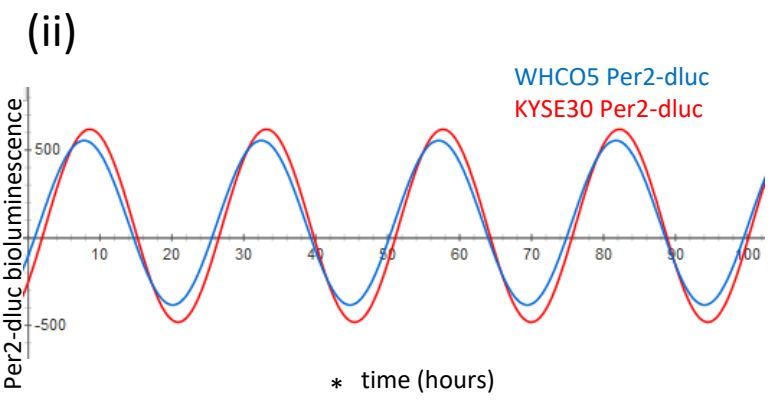
(ii)
WHCO5 Per2-dluc
KYSE30 Per2-dluc
Per2-dluc bioluminescence
time (hours)

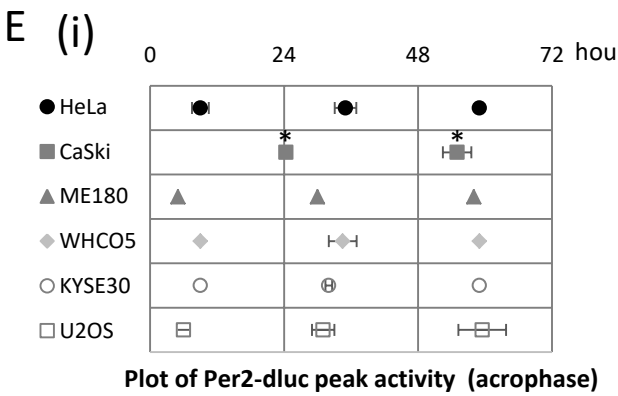
E
(i)
0 24 48 72 hours
HeLa
CaSki
ME180
WHCO5
KYSE30
U2OS
Plot of Per2-dluc peak activity (acrophase)

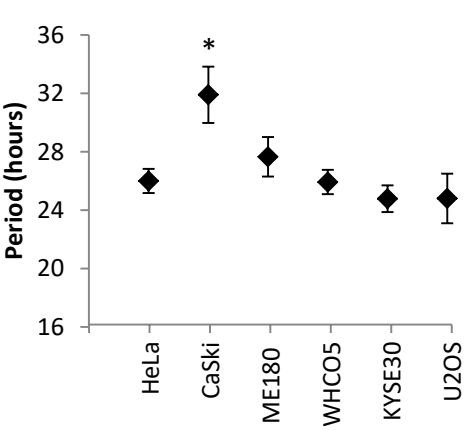
(ii)
Period (hours)
HeLa
CaSki
ME180
WHCO5
KYSE30
U2OS

Figure 6

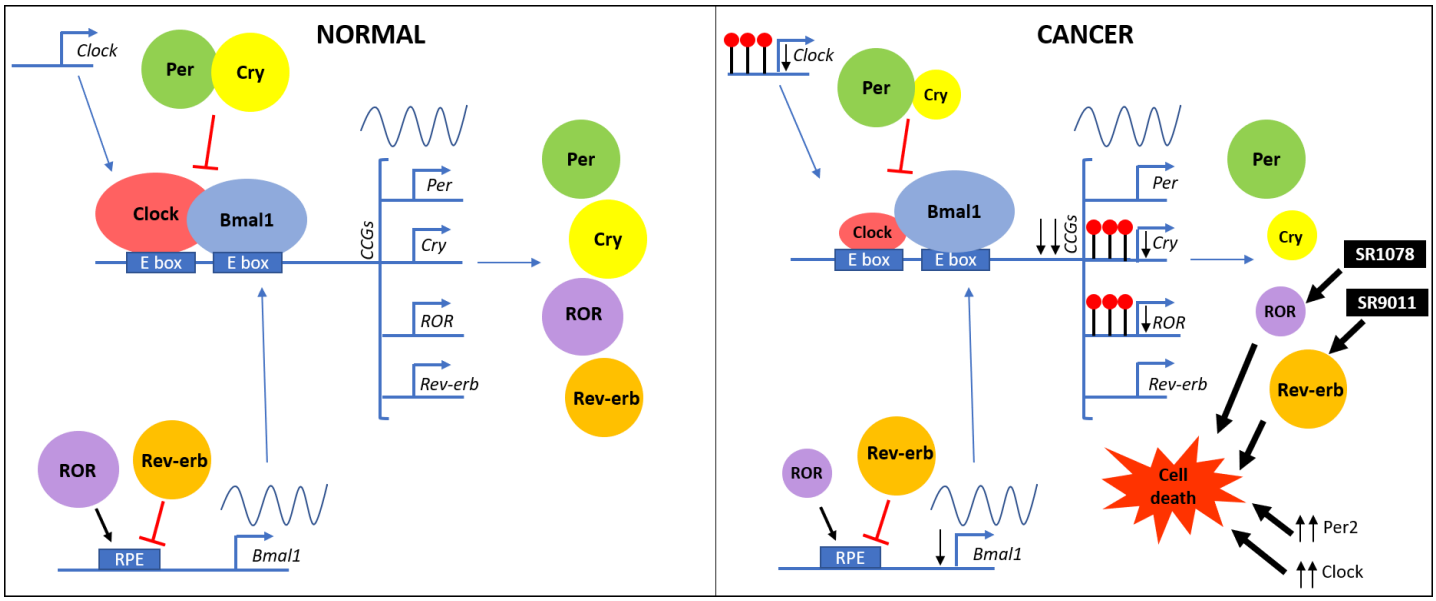
NORMAL
Clock
Per
Cry
Clock
Bmal1
E box
E box
CCGs
Per
Cry
ROR
Rev-erb
Per
Cry
ROR
Rev-erb
ROR
Rev-erb
RPE
Bmal1
CANCER
Clock
Per
Cry
Clock
Bmal1
E box
E box
CCGs
Per
Cry
ROR
Rev-erb
Per
Cry
ROR
SR1078
SR9011
Rev-erb
Cell death
Per2
Clock
ROR
Rev-erb
RPE
Bmal1

Table 1. Table showing primers used for methylation-specific PCR

Gene	Sequence	Annealing temperature (°C)
Clock-M Amplicon size: 150 bp Location: -1203 to -1054)	Forward: 5'- TTAGTAATCGGCGTCGTTTTCGGTC-3' Reverse: 5'- CGATACGCATACGACTTACCCCGTT-3'	55°C
Clock-UM Amplicon size: 148 bp Location: -1201 to -1054)	Forward: 5'- AGTAATTGGTGTTGTTTTTGGTTGG-3' Reverse: 5'- CAATACACATACAACTTACCCCATT-3'	52°C
RORα-M Amplicon size: 124 bp Location: -292 to -169)	Forward: 5'-GGCGGTTATAGGTGATTTCGAAGGC-3' Reverse: 5'-CGCGAACAAATAAATAACAACGACGAC-3'	55°C
RORα-UM Amplicon size: 122 bp Location: -290 to -169)	Forward: 5'-TGGTTATAGGTGATTTTGAAGGTGA-3' Reverse: 5'-CACAAACAAATAAATAACAACAACAAC-3'	52°C
Cry1-M Amplicon size: 122 bp Location: +11 to +132)	Forward: 5'-GGTAGTTTCGGGATCGGTTATCGG-3' Reverse: 5'-AAAATAAACCCCTATCGACGACGCT-3'	55°C
Cry1-UM Amplicon size: 124 bp Location: +10 to +133)	Forward: 5'-GGGTAGTTTTGGGATTGGTTATTGG-3' Reverse: 5'-AAAAATAAACCCCTATCAACAACACT-3'	52°C
Per2-M Amplicon size: 136 bp Location: +94 to +229)	Forward: 5'-GATTTTTCGGTTTGAAACGGCGTC-3' Reverse: 5'-GAAAATTCGAATCCCCAACCCTCG-3'	55°C
Per2-UM Amplicon size: 141 bp Location: +89 to +229)	Forward: 5'-TGTTGGATTTTTTGGTTTGAAATGGTGTT-3' Reverse: 5'-AAAAATTCAAATCCCCAACCCTCAAT-3'	52°C

The locations indicated are relative to the transcriptional start site at +1. M: methylated-specific primers, UM: unmethylated-specific primers.